**Figure S1. Immunolocalization of Avp and Oxt in the seabream pituitary gland.**

(A-E) Immunostaining of Avp (A-C) and Oxt (D-F) in paraffin sections of the posterior pituitary (neurohypophysis). In A and C and D and F, the epifluorescence image (red color) is merged with the brightfield image. **(C-F)** Control sections incubated with preabsorbed antisera. Scale bars, 200 µm (A, D, C and F); 50 µm (B and E).
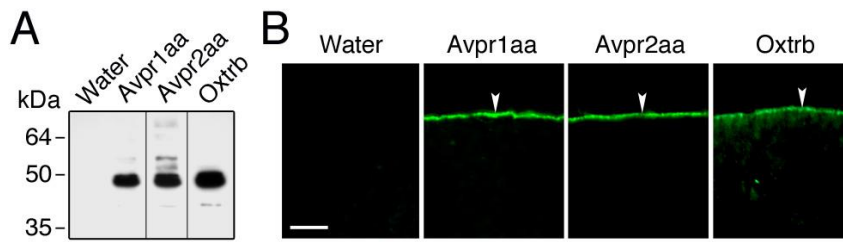
Figure S2. Expression of seabream Avp and Oxt receptors in *X. laevis* oocytes.

(A) Immunoblots of total membranes of oocytes injected with water or expressing HA-tagged Avpr1aa, Avpr2aa or Oxtrb. Molecular mass markers (kilodaltons) are on the left. **(B)** Immunofluoresence microscopy of water-injected and Avpr1aa-, Avpr2aa- or Oxtrb-expressing oocytes. The arrowhead points the oocyte plasma membrane. Scale bar, 50 µm.
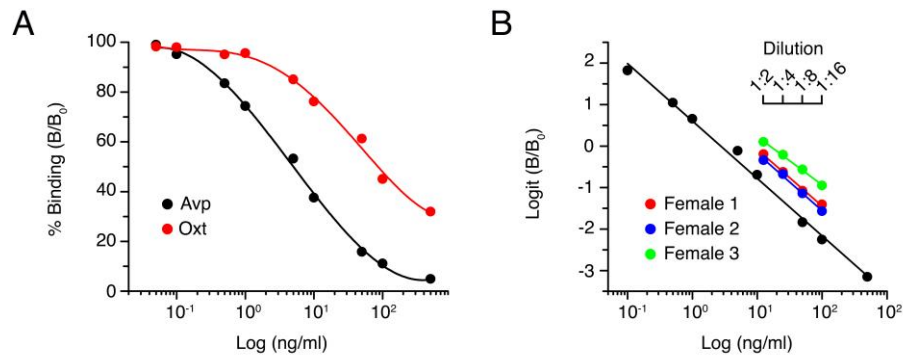
Figure S3. Development of an ELISA for Avp.

(A) Competitive binding curves for arginine vasopressin (Avp) standard, and cross-reactivity with serial dilutions of oxytocin (Oxt), using the anti-Avp antiserum. Data are the mean of 3 replicates. The optimal concentration for coating the wells with Avp was 50 ng/ml using a 1:15000 dilution of the antibody, whereas the Avp used to generate the standard curves ranged from 10 pg to 500 ng/ml. The sensitivity of the assay was 10 pg/ml (B/B0 > 95%) with the optical density decreasing as a linear function of Avp concentration (r^2 =0.9945). The intra- and inter-assay coefficient of variation was 4.64% and 8.35%, respectively. The evaluation of the cross-reactivity of the assay with Oxt showed that the displacement of the B/B0 dilution curve obtained with Avp was only seen when using high doses of Oxt (>10 ng/ml), the cross-reaction being 8.4%. **(B)** Parallelism between the standard curve of ELISA using Avp and displacement curves obtained with serial dilutions of the ovary from three different females. Each point is the mean of two replicates. The slope obtained for Avp (slope ± SEM) was of −0.588 ± 0.025 , and not significantly different from that obtained for ovarian samples from 3 different females (-0.566 ± 0.029).
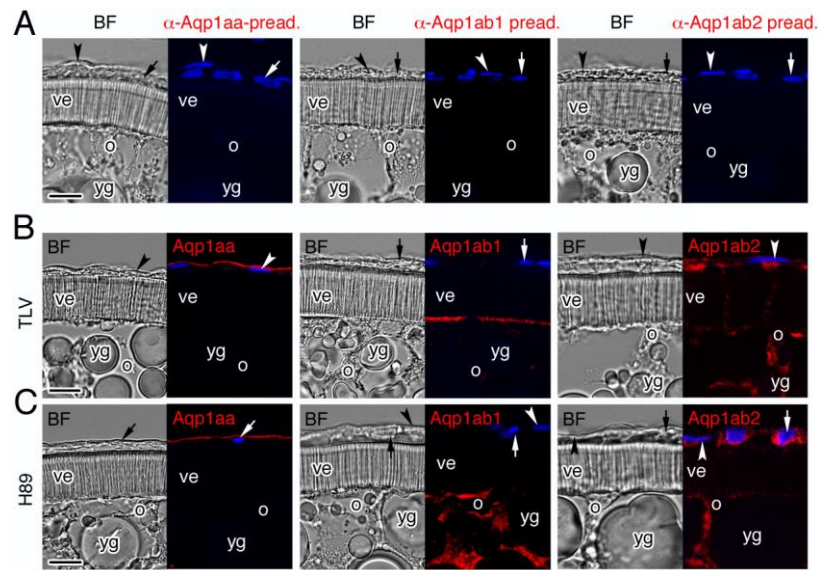
Figure S4. Immunostaining of the TSA1C channels in the seabream ovarian follicle.

(A) Control paraffin sections incubated with preabsorbed antisera specific for Aqp1aa, Aqp1ab1 and Aqp1ab2. **(B-C)** Representative immunostaining of Aqp1aa, Aqp1ab1 and Aqp1ab2 (red color) in follicles exposed only to 10 µM of the Avpr2aa antagonist tolvaptan (TLV) or the PKA inhibitor H89. In all panels, brightfield (BF) and epifluprescence images are shown on the left and right, respectively, and nuclei were counterstained with DAPI (blue). The theca and granulosa cells are indicated by arrows and arrowheads, respectively. ve, vitelline envelope; o, oocyte; yg, yolk globules. Scale bars, 10 µm.
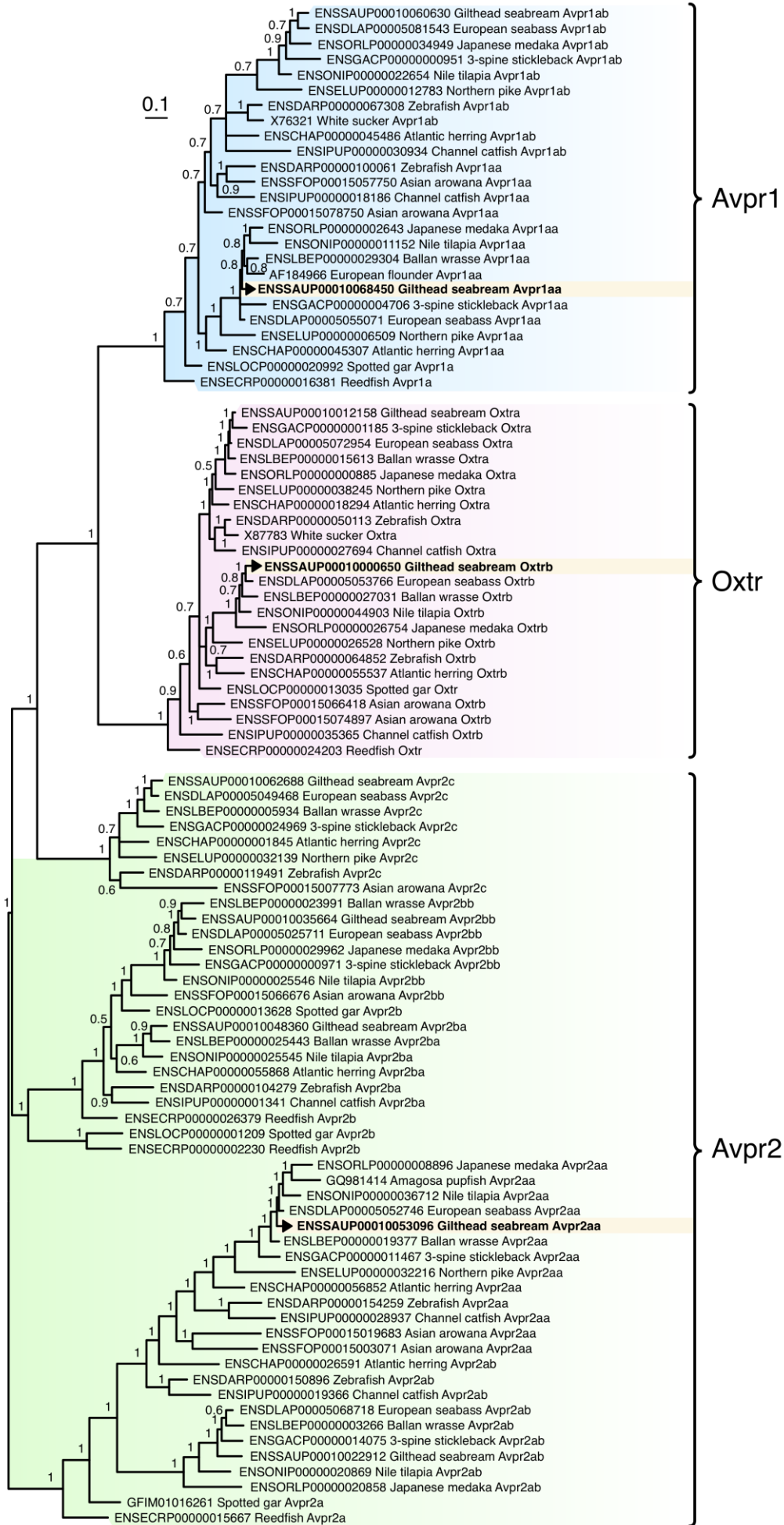
Figure S5: Molecular phylogeny of piscine vasopressinergic and oxytocinergic receptors.

Bayesian majority rule midpoint rooted consensus tree inferred from 2 million MCMC generations (aamodel = mixed4; burnin = 25%) of a ClustalX amino acid alignment of 97 receptors downloaded from Ensembl (v109). Bayesian posterior probabilities are shown at each node with the scale bar indicating the expected rate of amino acid substitution per site. The seabream paralogs used for functional experiments in the present study are highlighted (orange) with arrows in bold. The tree topology matches that computed by maximum likelihood (Daza et al., 2022) with the exception that the zebrafish Avpr2ba and Avpr2bb receptors are named in accordance with the Ensembl (v109) nomenclature.

Daza DO, Bergqvist CA, Larhammar D (2022) The evolution of oxytocin and vasotocin receptor genes in jawed vertebrates: A clear case for gene duplications through ancestral whole-genome duplications. Front Endocrinol 12: 792644.